

Adsorptive Removal of Methylene Blue from Aqueous Solution by Spent Mushroom Substrate: Equilibrium, Kinetics, and Thermodynamics

Tingguo Yan and Lijuan Wang*

Spent mushroom substrate (SMS), a renewable bio-waste from the mushroom-growing industry, was used as an adsorbent to remove methylene blue (MB) from aqueous solution. SMS was characterized using scanning electron microscopy (SEM) and Fourier-transform infrared spectroscopy (FTIR). Adsorption experiments with the SMS adsorbent were performed based on various parameters, such as adsorbent dose, initial MB dye concentration, initial pH, contact time, and temperature. The Langmuir, Freundlich, and Temkin isotherm models were employed to interpret the adsorption behavior. The results indicated that the equilibrium data were perfectly represented by the Temkin isotherm. The maximum adsorption capacity of SMS reached 63.5 mg g^{-1} at 303 K. The kinetics studies indicated that the pseudo-second-order model best described the adsorption of MB on SMS. The activation energy of the adsorption was 5.64 kJ mol^{-1} . Thermodynamic parameters suggested that the adsorption was an exothermic and spontaneous physical process. The results imply that SMS is a potentially low-cost adsorbent for treating wastewater containing cationic dyes.

Keywords: Adsorption; Methylene blue (MB); Spent mushroom substrate (SMS); Isotherm; Kinetics; Thermodynamics

Contact information: Key Laboratory of Bio-based Material Science and Technology of Ministry of Education, Northeast Forestry University, 26 Hexing Road, Harbin 150040, P. R. China;

* Corresponding author: donglinwlj@163.com

INTRODUCTION

Dyes are widely used in many industries, such as textiles, leather, cosmetics, paper, and printing plastics (Sharma *et al.* 2011). More than 10×10^5 commercially available dyes with over 7×10^5 tons of dyestuff are produced per year (Pearce 2003), and about 10 to 15% of the used dye is lost in the effluent of textile units (Dod *et al.* 2012; Husain 2006). Many dyes have toxic, carcinogenic, mutagenic, and teratogenic effects on aquatic life and also on humans (Bhattacharyya and Sharma 2005; Chatterjee *et al.* 2009). Additionally, dyes persist in water systems, causing aesthetic and environmental problems that affect water transparency and gas solubility (Papinutti and Forchiassi 2011). Therefore, the removal of such dyes from effluents prior to their final discharge is of significant environmental, technical, and commercial importance (Allen *et al.* 2004). The methodologies generally adopted to treat dye wastewater are classified in the following four categories: (I) physical, (II) chemical, (III) biological, and (IV) acoustical, radiation, and electrical processes (Gupta and Suhas 2009). Among these methods, adsorption is a well-known equilibrium separation process and an effective method for water decontamination applications (Hubbe *et al.* 2012). Activated carbon is the preferred adsorbent; however, its widespread application is restricted due to its high cost. Agricultural wastes are available in large amounts in nature. These materials have been potential adsorbents for dye-containing wastewater. Many previous studies of various dye

adsorptions using adsorbents based on agricultural wastes are listed in Table 1. However, dye-containing wastewater treatment based on SMS is rarely reported.

Table 1. Previous Studies of Various Dye Adsorptions Using Adsorbents Based on Agricultural Wastes

Adsorbents	Dyes	References
Neem sawdust	Malachite green	(Khattri and Singh 2009)
Cotton stalk	Methylene blue	(Ertas <i>et al.</i> 2010)
Eucalyptus bark	Basic red-12	(Khosla <i>et al.</i> 2012)
Garlic peel	Methylene blue	(Hameed and Ahmad 2009)
Azadirachta indica leaf	Congo red	(Bhattacharyya and Sharma 2004)
Tea waste	Janus green, methylene blue, thionine, crystal violet, congo red, neutral red and reactive blue 19	(Madrakian <i>et al.</i> 2012)
Peanut hull	Reactive black 5	(Tanyildizi 2011)
Rice husk	Neutral red	(Zou <i>et al.</i> 2009)
Wheat straw	Methylene blue	(Zhang <i>et al.</i> 2011)

Though mushroom growers often use a composted mixture as their growth medium for their product (Hubbe *et al.* 2010), such mixtures cannot be expected to have ideal properties for use as soil amendments, especially after having been used for the production of mushrooms. Hence, the utilization of such waste materials is most desirable. This study reports on the feasibility of utilizing SMS as a low-cost alternative adsorbent for the removal of MB from aqueous solution. The effects of adsorbent dose, initial dye concentration, initial pH, contact time, and temperature on MB adsorption onto SMS were investigated. Isotherm, kinetics, and thermodynamic parameters of the adsorption process were also investigated.

EXPERIMENTAL

Preparation of MB Solutions

Methylene blue (CAS: 61-73-4; $C_{16}H_{18}ClN_3S \cdot 3H_2O$; FW =373.90), a cationic basic dye, was supplied by Tianjin Kemiou Chemical Reagent Co., Ltd and used as an adsorbate. Stock solution was prepared by dissolving 0.5 g of MB in 1 L of distilled water. The solutions for use in experiments were obtained by diluting a stock solution of MB with distilled water to the desired concentration.

Preparation and Characterization of Adsorbent

SMS utilized in this work was collected in the summer of 2010 from Taoshan town in the Yichun forest district of Heilongjiang Province, China. The collected materials were thoroughly rinsed with running water several times to remove impurities, and they were then washed with distilled water. The clean SMS was dried in an oven at 85 °C for 6 h. The dried SMS was crushed and sieved to 60- to 80-mesh particles for further use in adsorption experiments.

Fourier transform infrared (FTIR) analysis was applied to determine the surface functional groups responsible for adsorption of the MB dye using a Nicolet 560 spectrometer (Nicolet Co., Ltd., USA), where the spectra were recorded in the range of 4000 to 400 cm^{-1} . The surface morphology was studied using a Quanta 200 scanning electron microscope with an accelerating voltage of 12.5 kV. 2012). The point of zero charge (pH_{PZC}) was determined by means of the solid addition method (Verma *et al.*

2012). The surface area and pore volume of SMS were calculated based on the nitrogen adsorption isotherm at 77 K, using measurements performed on an ASAP 2010 analyzer (Micromeritics, USA).

Experimental Methods

The batch adsorption experiments to evaluate the ability of SMS to remove MB dye from aqueous solution were carried out in 250-mL conical flasks containing 50-mL MB solutions in a water bath. The conical flasks were shaken at 110 rpm for the required time. The effect of solution pH on the removal of MB was investigated in the pH range from 2 to 10. The initial solution pH was adjusted using 0.1 M HCl or 0.1 M NaOH.

In the present study, adsorption equilibrium experiments were performed by stirring 50 mL of MB aqueous solution with a concentration of 80 mg L⁻¹ in each 250-mL conical flask containing 50 to 200 mg of SMS adsorbent at the original solution pH. The solutions were agitated at temperatures ranging from 303 K to 333 K. Adsorption kinetics experiments were conducted by keeping 100 mg of SMS adsorbent and 50 mL of an 80-mg L⁻¹ solution of MB dye in a series of 250-mL conical flasks at the original solution pH. The system was kept under stirring at temperatures ranging from 303 K to 333 K. The flasks were then taken out at intervals. At the end of each adsorption experiment, the adsorbent was removed by filtration through a 400-mesh nylon screen, and the dye concentration of the supernatant was analyzed using a UV-visible spectrophotometer by monitoring the absorbance changes at $\lambda_{\max} = 668$ nm.

The dye removal efficiency (R) and the amount of dye adsorbed per unit mass of adsorbent at time t (q_t , mg g⁻¹) and at equilibrium (q_e , mg g⁻¹), were calculated using the following equations,

$$R (\%) = [(C_0 - C_t) / C_0] \times 100 \quad (1)$$

$$q_t = (C_0 - C_t) V/W \quad (2)$$

$$q_e = (C_0 - C_e) V/W, \quad (3)$$

where C_t (mg L⁻¹) is the dye concentration at time t and C_0 and C_e (mg L⁻¹) are the initial and equilibrium dye concentrations, respectively. q_e (mg g⁻¹) represents the amount of dye adsorbed onto the adsorbent at equilibrium. V (mL) is the volume of the dye solution, and W (mg) is the mass of the adsorbent.

RESULTS AND DISCUSSION

Characterization of SMS

The infrared spectrum of SMS is shown in Fig. 1. The intense adsorption bands around 3500 to 3200 cm⁻¹ reveal the stretching vibrations of amino groups the hydroxyl groups (Akar *et al.* 2009; Bayramoğlu *et al.* 2006). The peak at a range from 3000 to 2800 cm⁻¹ can be attributed to C-H stretching vibrations. The weak peak at a range from 1725 to 1705 can be attributed to C=O stretching vibrations. The strong peak from 1650 to 1590 cm⁻¹ is due to N-H deformation vibration. The peak at 1322 cm⁻¹ is due to C-O vibrations in syringyl derivatives and the peak at 1250 cm⁻¹ is attributed to C-N stretching vibration. The peak at 1038 cm⁻¹ can be assigned to C-O stretching vibration in cellulose.

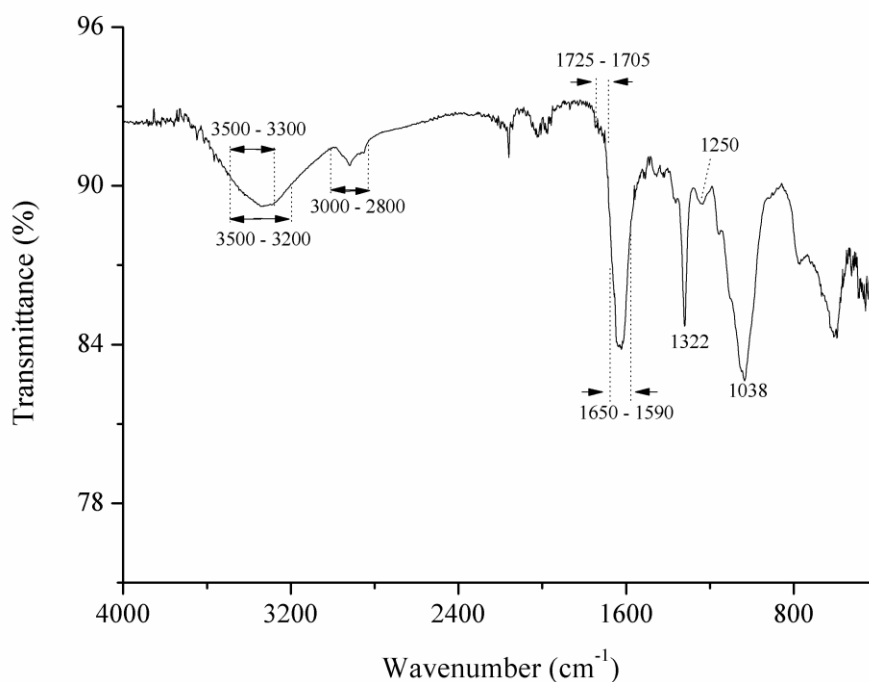


Fig. 1. FTIR spectrum of SMS

SEM micrographs of SMS are presented in Fig. 2. SMS consists of various biopolymers, such as lignin, cellulose, and hemicellulose, which are degraded and consumed by the fungus as carbon and energy sources, leading to many pores. These pores can be observed on the SMS surface in Fig. 2. These pores were 3 to 6 μm in diameter; therefore, most of them are classified as macropores. The BET surface area of the SMS particles was $2.417 \text{ m}^2 \text{ g}^{-1}$, indicating that the pores contributed little to the specific surface area.

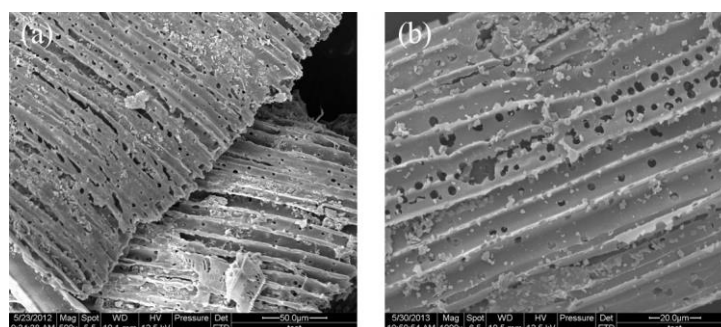


Fig. 2. SEM photographs of SMS at (a) 500x and (b) 1000x magnification

Effect of Initial pH

The pH of the initial solution is one of the most important factors influencing the adsorption of dyes on an adsorbent (Alencar *et al.* 2012; Crini *et al.* 2007). Figure 3(a) shows the effects of initial pH on the adsorption capacity and removal of MB dye. With pH increasing from 2 to 4, the removal and the adsorption capacity increased from 32.5% to 88.9% and from 13.0 mg g^{-1} to 35.5 mg g^{-1} , respectively. Further increasing the pH only improved the adsorption to a small extent. As illustrated in Fig. 3(b), the value of pH_{PZC} was around 6.5. Generally, the dissolved cationic dye is positively charged in aqueous solution. At low pH, the surface of the adsorbent gathers positive charges by adsorbing H^+ ions, which prevents the adsorption of cationic dye onto the adsorbent

surface due to electrostatic repulsion and the competition between H^+ ions and cationic dye for the adsorption sites (Senthil Kumar *et al.* 2010). The number of negatively charged surface sites on the adsorbent increased with increasing initial pH, which may lead to an increase in the adsorption of cationic dye due to the electrostatic attraction (Amin 2009). If electrostatic interaction was the only mechanism for MB adsorption, the adsorption capacity should still be low within the range pH from 4 to 6. In this pH range, the surface of SMS and dyes are positively charged. However, the experimental data from this study did not follow this prediction. The observed trend indicates that the electrostatic interaction was not the only mechanism for MB dye adsorption in the present system. The SMS can also interact with MB molecules via hydrogen bonding.

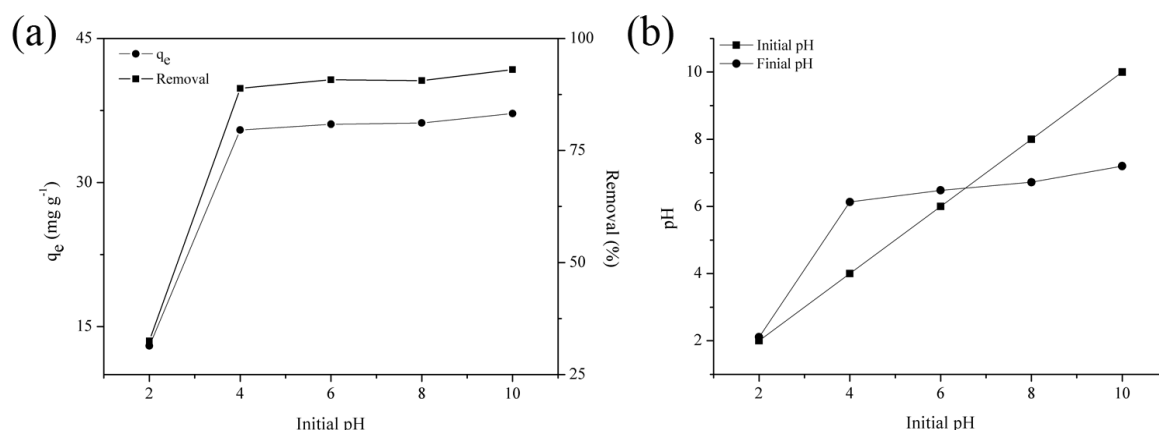


Fig. 3. Effect of initial solution pH (a) and final pH (b) on MB adsorption using SMS adsorbent (dye concentration: $80\ mg\ L^{-1}$; volume: $50\ mL$; temperature: $303\ K$; dose: $100\ mg$; time: $12\ h$)

Effects of SMS Dose and Temperature

The effects of adsorbent dose and temperature on MB adsorption are shown in Fig. 4. With increasing adsorbent dose, the adsorption capacity (q_e) for SMS decreased from $63.5\ mg\ g^{-1}$ to $9.6\ mg\ g^{-1}$ at $303\ K$. Similar trends are found at other temperatures. This phenomenon is due to the increased adsorbent surface area, *i.e.*, the high number of unsaturated adsorption sites occurring during the adsorption process (Alencar *et al.* 2012). With a decrease in temperature from 333 to $303\ K$, the adsorption capacity at equilibrium of MB adsorption onto SMS increased from 48.2 to $63.5\ mg\ g^{-1}$, revealing the exothermic nature of the adsorption, *i.e.*, a lower temperature favors the adsorption.

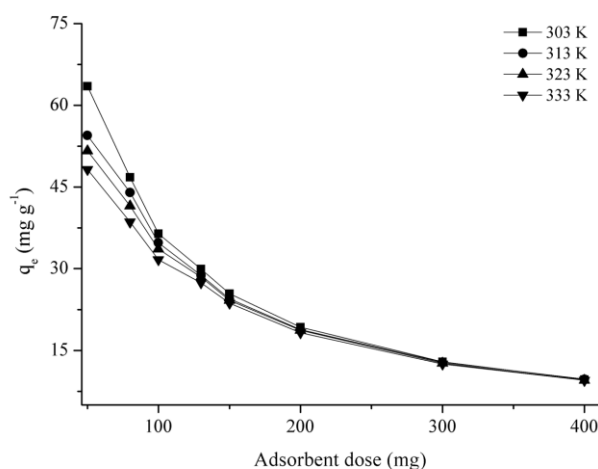


Fig. 4. Effect of adsorbent dose and temperature on MB adsorption (dye concentration: $80\ mg\ L^{-1}$; volume: $50\ mL$; time: $12\ h$)

Effects of Initial Concentration and Contact Time

The effects of initial dye concentration and contact time are shown in Fig. 5. The adsorption capacity (q_t) for SMS increases quickly within the initial 60 min and then gradually becomes slower as the equilibrium is attained. This is associated with the large number of vacant active surface sites on the SMS surface that are available at the initial stage of the adsorption. However, the remaining vacant active sites are less available for adsorption as time lapses because of the repulsive forces between the adsorbed and free molecules (de Sá *et al.* 2013). With an increase in the initial MB concentration from 40 to 100 mg L⁻¹, the adsorption capacity at equilibrium for SMS increased from 18.8 to 45 mg g⁻¹, which can be attributed to an increase in driving force for the mass transfer between the aqueous phase and solid phase (Senthil Kumar *et al.* 2010).

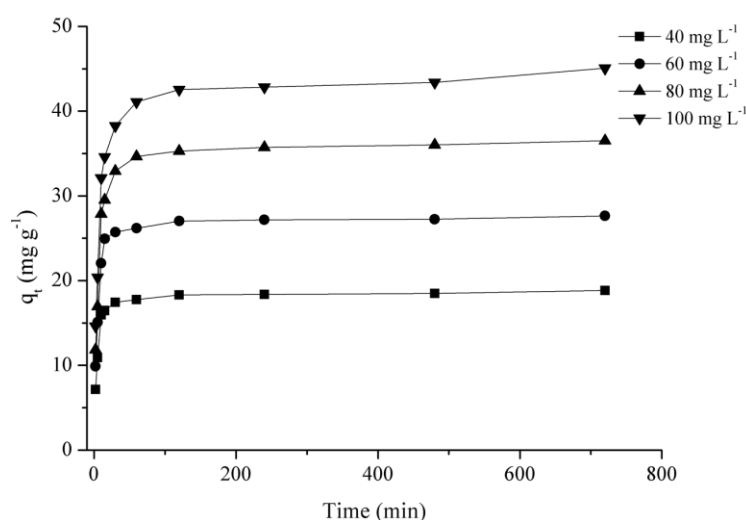


Fig. 5. Effect of initial dye concentration and contact time on MB adsorption (adsorbent dose: 100 mg; volume: 50 mL; temperature: 303 K)

Adsorption Isotherm Studies

Langmuir, Freundlich, and Temkin isotherm models were employed to analyze the equilibrium data obtained.

The linear form of the Langmuir isotherm model (Langmuir 1918) can be given as,

$$C_e/q_e = 1/(bq_m) + C_e/q_m, \quad (4)$$

where C_e (mg L⁻¹) is the equilibrium dye concentration, q_e (mg g⁻¹) represents the amount of dye adsorbed onto the adsorbent at equilibrium, and q_m (mg g⁻¹) and b (L mg⁻¹) are the maximum monolayer capacity of the adsorbent and the Langmuir isotherm constant, respectively. The plot of C_e/q_e versus C_e gives a linear relationship, as shown in Fig. 6(a). The parameters b and q_m were calculated from the intercept and slope, respectively, and their values at various temperatures are listed in Table 2. As shown in Table 2, R^2 values at different temperatures were determined to be in the range of 0.8323 to 0.9635. Moreover, q_m calculated from the Langmuir isotherm was far higher than the experimental value. Therefore, the Langmuir model does not describe the adsorption of MB onto SMS.

The Freundlich model (Freundlich 1985) can be expressed as,

$$\ln q_e = \ln K_f + (1/n_f)\ln C_e, \quad (5)$$

where K_f ($(\text{mg g}^{-1})(\text{mg L}^{-1})^{-1/n}$) is the Freundlich constant and $1/n_f$ (dimensionless) is the heterogeneity factor. Figure 6(b) shows the plot of $\ln q_e$ against $\ln C_e$, and n_f and K_f can be calculated from the slope and intercept of the plot, respectively. The results are presented in Table 2. The correlation coefficients (R^2) are higher than those of the Langmuir model (> 0.96), which confirms that the experimental data can be well described by the Freundlich model. The n_f value is above 1.2, which illustrates that MB is favorably adsorbed onto SMS (Rauf *et al.* 2008).

The Temkin isotherm (Temkin and Pyzhev 1940) model can be shown in linear form as follows,

$$q_e = (RT/b_T) \ln A_T + (RT/b_T) \ln C_e \quad (6)$$

where A_T (L g^{-1}) and b_T (J mol^{-1}) are the Temkin constants. The values of A_T and b_T can be calculated from the intercept and the slope of the linear plots obtained by plotting q_e versus $\ln C_e$ in Fig. 6(c), respectively, and the results are listed in Table 2. The linear regression correlation coefficients (R^2) are higher than those of the other isotherms, *i.e.*, the equilibrium data can be better interpreted by the Temkin isotherm than the other isotherms, suggesting a uniform distribution of binding energy arising due to interaction of the dye molecules.

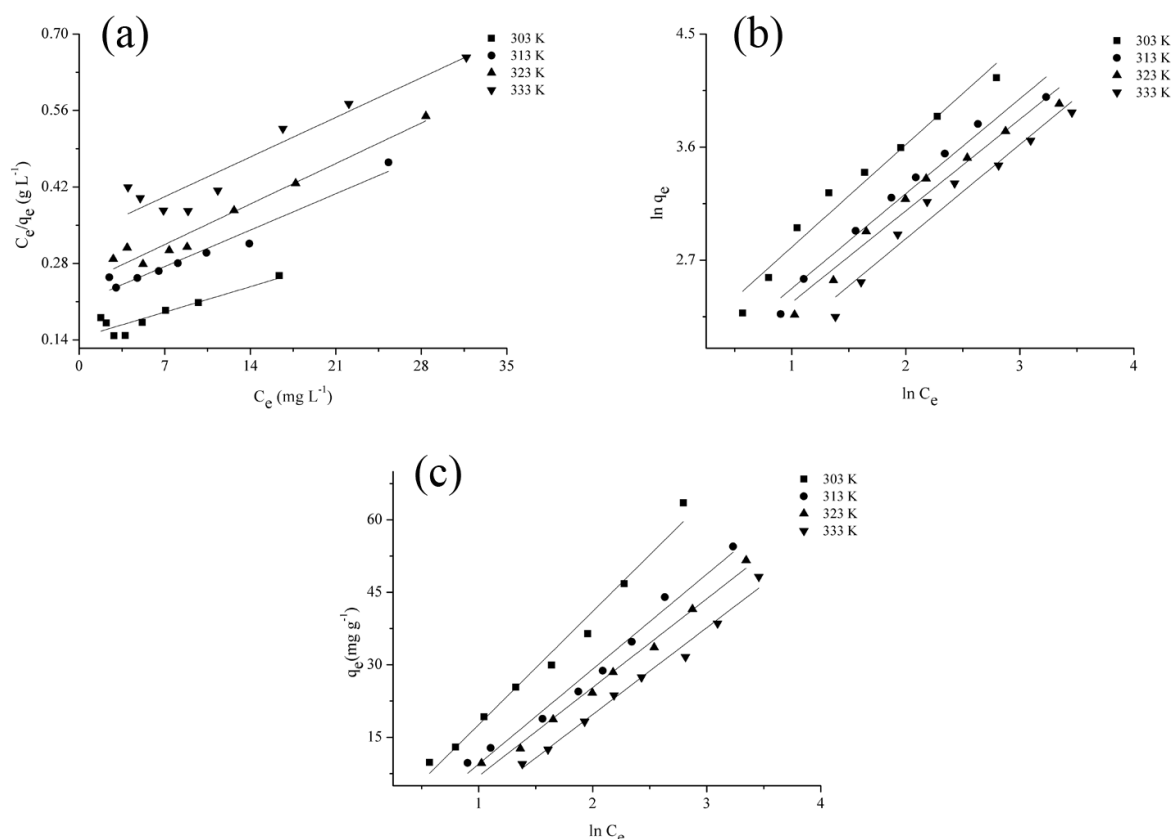


Fig. 6. The linear plots of the (a) Langmuir, (b) Freundlich, and (c) Temkin equilibrium models

Adsorption Kinetics Studies

Pseudo-first-order, pseudo-second-order, and intra-particle diffusion kinetics models were selected to fit the experimental kinetics data. The linear plots and constants of all kinetics models are shown in Fig. 7 and Table 3, respectively.

The mathematical forms of the pseudo-first order model (Lagergren 1898) and the pseudo-second order model (Ho and McKay 1999) can be defined as in Eq. (7) and Eq. (8), respectively,

$$1/q_t = k_1/(q_e t) + 1/q_e \quad (7)$$

$$t/q_t = 1/(k_2 q_e^2) + t/q_e, \quad (8)$$

where k_1 (min^{-1}) and k_2 ($\text{g mg}^{-1} \text{min}^{-1}$) are the pseudo-first-order and the pseudo-second-order rate constants, respectively, and q_t (mg g^{-1}) and q_e (mg g^{-1}) are the amounts of MB adsorbed per unit weight of SMS at time t (min) and at equilibrium, respectively.

Table 2. Equilibrium Constants for MB Adsorption on SMS

Isotherm Models	303 K	313 K	323 K	333 K
Langmuir				
q_m (mg g^{-1})	149.25	105.26	94.34	96.15
b (L mg^{-1})	0.046	0.046	0.044	0.032
R^2	0.8323	0.9607	0.9635	0.9051
Freundlich				
n_f	1.228	1.325	1.373	1.333
K_f (mg g^{-1})(mg L^{-1}) $^{-1/n}$	7.318	5.590	5.138	3.938
R^2	0.9657	0.9750	0.9691	0.9618
Temkin				
A_T (L mg^{-1})	0.7811	0.5960	0.5384	0.4053
b_T (J mol^{-1})	107.65	132.52	146.44	154.06
R^2	0.9822	0.9841	0.9914	0.9879

The linear plots of $1/q_t$ versus $1/t$ and t/q_t against t are shown in Fig. 7(a) and Fig. 7(b), respectively. The values of q_e , k_1 , and k_2 can be determined from the slopes and intercepts of the plots. Although the correlation coefficients (R^2) at 303 K for the pseudo-first-order model are quite high (> 0.98), the calculated q_e ($q_{e,cal.}$) value is less accurate than that of the pseudo-second order model, *i.e.*, the calculated value of q_e ($q_{e,cal.}$) obtained in the pseudo-second order model perfectly agrees with the experimental values of q_e ($q_{e,exp.}$), indicating the experimental kinetics data is better described by the pseudo-second order model than the pseudo-first order model. The same observations were found at other temperatures studied. The results show that the rate-limiting step may be the adsorption mechanism.

The intra-particle diffusion model (Weber and Morris 1963) proposed by Weber and Morris can be described as,

$$q_t = k_{id}t^{1/2} + C, \quad (9)$$

where k_{id} ($\text{mg g}^{-1} \text{min}^{-1/2}$) is the intra-particle diffusion rate constant and C is a constant that gives information about the thickness of the boundary layer, *i.e.*, the larger the intercept, the greater is the boundary layer effect (Kannan and Sundaram 2001). The plot of q_t versus $t^{1/2}$ is presented in Fig. 7(c). The values of the intra-particle diffusion kinetics model parameters, k_{id} and C , are obtained from the slope and intercept of the plot, respectively, and listed in Table 3. It is essential for the plots to pass through the origin if the intra-particle diffusion is the rate-limiting step (Huang *et al.* 2011). The value of q_t increases quickly in the beginning and then increases slowly, indicating that the adsorption of MB on SMS is a multi-step process, with adsorption on the external surface, diffusion into the interior, and the final equilibrium stage included. As shown in Fig. 7(c), the adsorption process can be divided into two steps that are ascribed to the intra-particle diffusion stage and equilibrium stage because the step of adsorption on the external

surface is fast and less obvious. As the first linear plot corresponding to the intra-particle diffusion stage does not cross the origin, some degree of boundary layer control exists, which further shows that the intra-particle diffusion is not the only rate-controlling step; the other processes may control the rate of adsorption (Crini *et al.* 2008).

The activation energy can be determined by the Arrhenius equation (Wu 2007),

$$\ln k_2 = \ln A - E_a/RT \quad (18)$$

where k_2 ($\text{g mg}^{-1} \text{min}^{-1}$) is the pseudo-second order rate constant, A is the Arrhenius factor, and E_a (kJ mol^{-1}) is the activation energy. The parameters can be calculated from the slope of the linear plot of $\ln k_2$ versus $1/T$. The magnitude of activation energy (E_a) gives an idea about the type of adsorption, which is mainly physical or chemical. The physical process normally has an activation energy of 5 to 40 kJ mol^{-1} , while the chemical process has a higher activation energy of 40 to 800 kJ mol^{-1} (Nollet *et al.* 2003). In this study, the E_a value is 5.64 kJ mol^{-1} , which indicates a physical adsorption process.

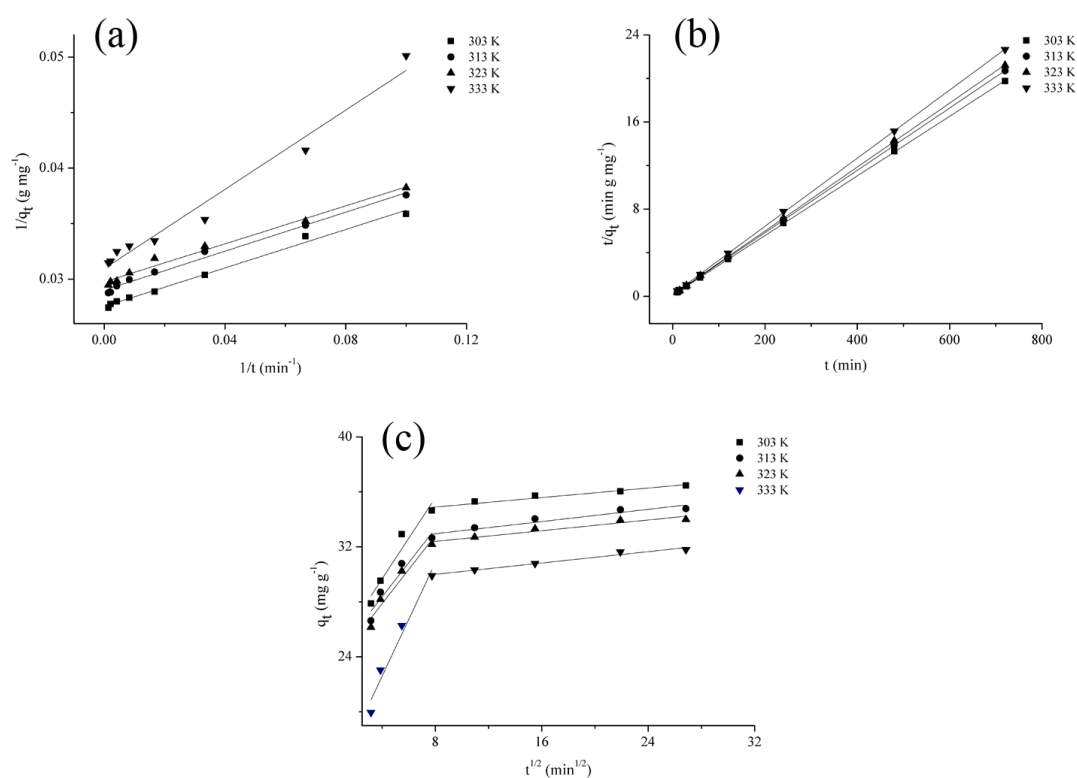


Fig. 7. The linear plots of the (a) pseudo-first order, (b) pseudo-second order, and (c) intra-particle diffusion kinetics models

Thermodynamic Parameters

Thermodynamic studies of the adsorption of MB onto SMS were performed at temperatures of 303, 313, 323, and 333 K. The parameters, including ΔG^0 , ΔH^0 , and ΔS^0 , were determined by the following equations,

$$\Delta G^0 = \Delta H^0 - T\Delta S^0 \quad (10)$$

$$\ln k_c = -(\Delta H^0/RT) + \Delta S^0/R \quad (11)$$

$$k_c = C_s/C_e \quad (12)$$

where ΔG^0 (kJ mol^{-1}), ΔH^0 (kJ mol^{-1}), and ΔS^0 ($\text{J mol}^{-1} \text{K}^{-1}$) are the standard free energy change, enthalpy change, and entropy change, respectively, and k_c and C_s (mg L^{-1}) are the equilibrium constant and the amount adsorbed on the solid at equilibrium, respectively.

Table 3. Kinetics Parameters for MB Adsorption

Kinetic Models	303 K	313 K	323 K	333 K
$q_{e,exp.}$ (mg g^{-1})	36.46	34.77	33.94	31.79
Pseudo-first order				
k_1 (min^{-1})	3.153	3.028	2.869	5.776
$q_{e,cal.}$ (mg g^{-1})	36.36	34.48	33.56	32.36
R^2	0.9928	0.9902	0.9860	0.9769
Pseudo-second order				
k_2 ($\text{g mg}^{-1} \text{min}^{-1}$)	0.007	0.007	0.007	0.006
$q_{e,cal.}$ (mg g^{-1})	36.50	34.96	34.01	31.95
R^2	1.000	1.000	1.000	1.000
Intra-particle diffusion				
k_{id1} ($\text{mg g}^{-1} \text{min}^{-1/2}$)	1.4718	1.2407	1.2435	2.0651
C (mg g^{-1})	23.79	23.402	22.89	14.33
R^2	0.9376	0.9397	0.9466	0.9653
k_{id2} ($\text{mg g}^{-1} \text{min}^{-1/2}$)	0.0867	0.111	0.0975	0.1002
C (mg g^{-1})	34.194	32.064	31.612	29.224
R^2	0.940	0.918	0.9324	0.9167

The values of ΔH^0 and ΔS^0 are estimated from the slope and intercept, respectively, of a plot of $\ln k_c$ against $1/t$. The results are summarized in Table 4. The negative values of ΔG^0 and ΔH^0 suggest that MB adsorption is a spontaneous and exothermic process. The magnitude of the standard enthalpy changes for absolute physical adsorption is less than 20 kJ mol^{-1} , while chemisorption is in the range of 80 to 200 kJ mol^{-1} (Gu *et al.* 1994). In this study, the magnitude of standard enthalpy changes ($|\Delta H^0|$) for SMS is determined to be 25.82, indicating the contribution of both adsorption types. Because the magnitude of the standard enthalpy changes ($|\Delta H^0|$) was a little higher than 20, the adsorption process is dominated by physical adsorption, which is consistent with the result from the activation energy study.

Table 4. Thermodynamic Data for MB Adsorption

R^2	ΔH^0 (kJ mol^{-1})	ΔS^0 ($\text{J mol}^{-1} \text{K}^{-1}$)	ΔG^0 (kJ mol^{-1})			
			303 K	313 K	323 K	333 K
0.9767	-25.82	-66.00	-5.81	-5.15	-4.49	-3.83

CONCLUSIONS

In this study, SMS as a natural adsorbent was investigated for the removal of MB from aqueous solution in batch experiments.

1. The equilibrium data fit well with the Temkin isotherm. The maximum adsorption capacity of MB adsorption on SMS was 63.5 mg g^{-1} at 303 K.

2. The amount of MB adsorbed on SMS increased as the initial concentration increased and as the pH increased in the range of 2 to 4. The higher adsorption capacity occurred in the pH range of 4 to 10. The pH effects suggest that the electrostatic attraction is not the only mechanism for MB dye adsorption in the present system.

3. The pseudo-second-order model best represented the kinetics data. The adsorption is a physical process because the E_a value was found as 5.64 kJ mol⁻¹. The thermodynamic parameters indicate that the adsorption is an exothermic and spontaneous process because both ΔG° and ΔH° values are negative. SMS is a potentially low-cost alternative for treating wastewater containing cationic dyes.

ACKNOWLEDGMENTS

The authors gratefully acknowledge support from the Fundamental Research Funds for the Central Universities (DL12DB04).

REFERENCES CITED

- Akar, S. T., Gorgulu, A., Kaynak, Z., Anilan, B., and Akar, T. (2009). "Biosorption of reactive Blue 49 dye under batch and continuous mode using a mixed biosorbent of macro-fungus *Agaricus bisporus* and *Thuja orientalis* cones," *Chemical Engineering Journal* 148(1), 26-34.
- Alencar, W. S., Acayanka, E., Lima, E. C., Royer, B., de Souza, F. E., Lameira, J., and Alves, C. N. (2012). "Application of *Mangifera indica* (mango) seeds as a biosorbent for removal of Victazol Orange 3R dye from aqueous solution and study of the biosorption mechanism," *Chemical Engineering Journal* 209(15), 577-588.
- Allen, S. J., McKay, G., and Porter, J. F. (2004). "Adsorption isotherm models for basic dye adsorption by peat in single and binary component systems," *Journal of Colloid and Interface Science* 280(2), 322-333.
- Amin, N. K. (2009). "Removal of direct blue-106 dye from aqueous solution using new activated carbons developed from pomegranate peel: Adsorption equilibrium and kinetics," *Journal of Hazardous Materials* 165(1-3), 52-62.
- Bayramoğlu, G., Çelik G., and Arica M. Y. (2006). "Biosorption of Reactive Blue 4 dye by native and treated fungus *Phanerocheate chrysosporium*: Batch and continuous flow system studies," *Journal of Hazardous Materials* 137(3), 1689-1697
- Bhattacharyya, K., and Sharma, A. (2005). "Kinetics and thermodynamics of methylene blue adsorption on neem (*Azadirachta indica*) leaf powder," *Dyes and Pigments* 65(1), 51-59.
- Bhattacharyya, K. G., and Sharma, A. (2004). "Azadirachta indica leaf powder as an effective biosorbent for dyes: A case study with aqueous Congo Red solutions," *Journal of Environmental Management* 71(3), 217-229.
- Chatterjee, S., Lee, D. S., Lee, M. W., and Woo, S. H. (2009). "Congo Red adsorption from aqueous solutions by using chitosan hydrogel beads impregnated with nonionic or anionic surfactant," *Bioresource Technology* 100(17), 3862-3868.
- Crini, G., Peindy, H., Gimbert, F., and Robert, C. (2007). "Removal of C.I. Basic Green 4 (Malachite Green) from aqueous solutions by adsorption using cyclodextrin-based adsorbent: Kinetic and equilibrium studies," *Separation and Purification Technology* 53(1), 97-110.
- Crini, G., Gimbert, F., Robert, C., Martel, B., Adam, O., Morin-Crini, N., De Giorgi, F., and Badot, P. M. (2008). "The removal of Basic Blue 3 from aqueous solutions by chitosan-based adsorbent: Batch studies," *Journal of Hazardous Materials* 153(1-2), 96-106.
- de Sá, F. P., Cunha, B. N., and Nunes, L. M. (2013). "Effect of pH on the adsorption of Sunset Yellow FCF food dye into a layered double hydroxide (CaAl-LDH-NO₃)," *Chemical Engineering Journal* 215-216(15), 122-127.

- Dod, R., Banerjee, G., and Saini, S. (2012). "Adsorption of methylene blue using green pea peels (*Pisum sativum*): A cost-effective option for dye-based wastewater treatment," *Biotechnology and Bioprocess Engineering* 17(4), 862-874.
- Ertas, M., Acemioglu, B., Alma, M. H., and Usta, M. (2010). "Removal of methylene blue from aqueous solution using cotton stalk, cotton waste and cotton dust," *Journal of Hazardous Materials* 183(1-3), 421-427.
- Freundlich, H. (1985). "Über die Adsorption in Lösungen," *The Journal of Physical Chemistry* 57, 387-470.
- Gu, B., Schmitt, J., Chen, Z., Liang, L., and McCarthy, J. F. (1994). "Adsorption and desorption of natural organic matter on iron oxide: Mechanisms and models," *Environmental Science & Technology* 28(1), 38-46.
- Gupta, V. K., and Suhas. (2009). "Application of low-cost adsorbents for dye removal--A review," *Journal of Environmental Management* 90(8), 2313-2342.
- Hameed, B. H., and Ahmad, A. A. (2009). "Batch adsorption of methylene blue from aqueous solution by garlic peel, an agricultural waste biomass," *Journal of Hazardous Materials* 164(2-3), 870-875.
- Huang, X. Y., Bu, H. T., Jiang, G. B., and Zeng, M. H. (2011). "Cross-linked succinyl chitosan as an adsorbent for the removal of Methylene Blue from aqueous solution," *International Journal of Biological Macromolecules* 49(4), 643-651.
- Hubbe, M. A., Nazhad, M., and Sánchez, C. (2010). "Composting as a way to convert cellulosic biomass and organic waste into high-value soil amendments: A review," *BioResources* 5(4), 2808-2854.
- Hubbe, M. A., Beck, K. R., O'Neal, W. G., and Sharma, Y. C. (2012). "Cellulosic substrates for removal of pollutants from aqueous systems: A review. 2. Dyes," *BioResources* 7(2), 2592-2687.
- Ho, Y. S., and McKay, G. (1999). "Pseudo-second order model for sorption processes," *Process Biochemistry* 34(5), 451-465.
- Husain, Q. (2006). "Potential applications of the oxidoreductive enzymes in the decolorization and detoxification of textile and other synthetic dyes from polluted water: A review," *Critical Reviews in Biotechnology* 26(4), 201-221.
- Kannan, N., and Sundaram, M. M. (2001). "Kinetics and mechanism of removal of methylene blue by adsorption on various carbons—A comparative study," *Dyes and Pigments* 51(1), 25-40.
- Khattri, S. D., and Singh, M. K. (2009). "Removal of malachite green from dye wastewater using neem sawdust by adsorption," *Journal of Hazardous Materials* 167(1-3), 1089-1094.
- Khosla, E., Kaur, S., and Dave, P. N. (2012). "Adsorption mechanism of Basic Red-12 over eucalyptus bark and its surface derivatives," *Journal of Chemical & Engineering Data* 57(7), 2004-2011.
- Lagergren, S. (1898). "Zur Theorie der sogenannten Adsorption gelöster Stoffe," *Kungliga Svenska Vetenskapsakademiens Handlingar* 24(4), 1-39.
- Langmuir, I. (1918). "The adsorption of gases on plane surfaces of glass, mica and platinum," *Journal of the American Chemical Society* 40(9), 1361-1403.
- Madrakian, T., Afkhami, A., and Ahmadi, M. (2012). "Adsorption and kinetic studies of seven different organic dyes onto magnetite nanoparticles loaded tea waste and removal of them from wastewater samples," *Spectrochimica Acta Part A: Molecular and Biomolecular Spectroscopy* 99(15), 102-109.
- Nollet, H., Roels, M., Lutgen, P., Van der Meer, P., and Verstraete, W. (2003). "Removal of PCBs from wastewater using fly ash," *Chemosphere* 53(6), 655-665.

- Papinutti, L., and Forchiassin, F. (2011). "Adsorption and decolorization of dyes using solid residues from *Pleurotus ostreatus* mushroom production," *Biotechnology and Bioprocess Engineering* 15(6), 1102-1109.
- Pearce, C. (2003). "The removal of colour from textile wastewater using whole bacterial cells: A review," *Dyes and Pigments* 58(3), 179-196.
- Rauf, M. A., Bukallah, S. B., Hamour, F. A., and Nasir, A. S. (2008). "Adsorption of dyes from aqueous solutions onto sand and their kinetic behavior," *Chemical Engineering Journal* 137(2), 238-243.
- Senthil Kumar, P., Ramalingam, S., Senthamarai, C., Niranjanaa, M., Vijayalakshmi, P., and Sivanesan, S. (2010). "Adsorption of dye from aqueous solution by cashew nut shell: Studies on equilibrium isotherm, kinetics and thermodynamics of interactions," *Desalination* 261(1-2), 52-60.
- Sharma, P., Kaur, H., Sharma, M., and Sahore, V. (2011). "A review on applicability of naturally available adsorbents for the removal of hazardous dyes from aqueous waste," *Environmental Monitoring and Assessment* 183(1-4), 151-195.
- Tanyildizi, M. Ş. (2011). "Modeling of adsorption isotherms and kinetics of reactive dye from aqueous solution by peanut hull," *Chemical Engineering Journal* 168(3), 1234-1240.
- Temkin, M. J., and Pyzhev, V. (1940). "Kinetics of ammonia synthesis on promoted iron catalysts," *Acta Physiochim. URSS* 12(3), 217-222.
- Verma, A. K., Dash, R. R., and Bhunia, P. (2012). "A review on chemical coagulation/flocculation technologies for removal of colour from textile wastewaters," *Journal of Environmental Management*, 93(1), 154-168.
- Weber, W. J., and Morris, J. C. (1963). "Kinetics of adsorption on carbon from solution," *Journal of the Sanitary Engineering Division* 89(2), 31-60.
- Wu, C. H. (2007). "Adsorption of reactive dye onto carbon nanotubes: Equilibrium, kinetics and thermodynamics," *Journal of Hazardous Materials* 144(1-2), 93-100.
- Zhang, W., Yan, H., Li, H., Jiang, Z., Dong, L., Kan, X., Yang, H., Li, A., and Cheng, R. (2011). "Removal of dyes from aqueous solutions by straw based adsorbents: Batch and column studies," *Chemical Engineering Journal* 168(3), 1120-1127.
- Zou, W., Han, P., Li, Y., Liu, X., He, X., and Han, R. (2009). "Equilibrium, kinetic and mechanism study for the adsorption of neutral red onto rice husk," *Desalination and Water Treatment* 12(1-3), 210-218.

Article submitted: July 2, 2013; Peer review completed: July 24, 2013; Revised version received and accepted: July 27, 2013; Published: July 30, 2013.